Diabetes Publish Ahead of Print, published online July 8, 2009

Vasohibin-1, a negative feedback regulator of angiogenesis, ameliorates renal alterations in a mouse model of diabetic nephropathy

Tatsuyo Nasu[1], Yohei Maeshima[1], Masaru Kinomura[1], Kumiko Hirokoshi-Kawahara[1], Katsuyuki Tanabe[1], Hitoshi Sugiyama[1, 2], Hikaru Sonoda[3], Yasufumi Sato[4] and Hirofumi Makino[1].

[1]Department of Medicine and Clinical Science, [2]Center for Chronic Kidney Disease and Peritoneal Dialysis, Okayama University Graduate School of Medicine, Dentistry and Pharmaceutical Sciences, Okayama, Japan; [3]Discovery Research Laboratories, Shionogi, Osaka, Japan and [4]Department of Vascular Biology, Institute of Development, Aging, and Cancer, Tohoku University, Sendai, Japan.

Address for Correspondence:
Dr. Yohei Maeshima,
E-Mail: ymaeshim@md.okayama-u.ac.jp

Additional information for this article can be found in an online appendix at
http://diabetes.diabetesjournals.org

Submitted 24 December 2008 and accepted 26 June 2009.

Objective: The involvement of pro-angiogenic factors such as VEGF as well as the therapeutic efficacy of angiogenesis inhibitors in early diabetic nephropathy has been reported. Vasohibin-1 is a unique endogenous angiogenesis inhibitor that is induced in endothelial cells by pro-angiogenic factors. Here, we investigated the therapeutic efficacy of vasohibin-1 (VASH-1) in an early diabetic nephropathy model.

Research Design and Methods: Streptozotocin-induced type 1 diabetic mice received intravenous injections of adenoviral vectors encoding VASH-1 (AdhVASH-1) or β-gal (AdLacZ) every other week, and were sacrificed after 28 days.

Results: Treatment with AdhVASH-1 resulted in sustained increase in the protein levels of VASH-1 in the liver and sera, in the absence of any inflammatory alterations. AdhVASH-1 treatment significantly suppressed renal hypertrophy, glomerular hypertrophy, glomerular hyperfiltration, albuminuria, increase of the $CD31^+$ glomerular endothelial area, $F4/80^+$ monocyte/macrophage infiltration, the accumulation of type IV collagen and mesangial matrix compared with AdLacZ-treated diabetic mice. Increase in the renal levels of TGF-β1, MCP-1 and RAGE in diabetic animals was significantly suppressed by AdhVASH-1 (real-time PCR and immunoblot). Vasohibin-1 also significantly suppressed the increase of TGF-β, MCP-1 and RAGE induced by high ambient glucose in cultured mouse mesangial cells. Increased phosphorylation of VEGFR2 was suppressed in AdVASH-1-treated diabetic animals, and in cultured glomerular endothelial cells. Endogenous mouse VASH-1 was localized to the mesangial and endothelial area in glomeruli of diabetic mice.

Conclusions: These results suggest the potential therapeutic efficacy of VASH-1 in treating early diabetic nephropathy potentially mediated via glomerular endothelial and mesangial cells.

Diabetic nephropathy is a major microvascular complication of type 1 and 2 diabetes, and 30-40% of patients with type 2 diabetes develop diabetic nephropathy. Since diabetic nephropathy is the most common pathological disorder predisposing end-stage renal disease (ESRD) in Japan and in the Western World, novel therapeutic approaches are required. In the early stage of diabetic nephropathy, glomerular hyperfiltration, glomerular and tubular epithelial hypertrophy, microalbuminuria and thickening of the glomerular basement membrane are typically observed. Then, expansion of the extracellular matrix (ECM) in mesangial areas and overt proteinuria are observed, eventually leading to glomerulosclerosis and ESRD(1). The involvement of various factors and cytokines including the renin-angiotensin system, insulin-like growth factor-I, monocyte chemoattractant protein-1 (MCP-1), fibrogenic transforming growth factor-β1 (TGF-β1), protein kinase C and advanced glycation end products (AGE) in diabetic nephropathy has been reported(2; 3).

Angiogenesis is associated with pathological conditions including tumor growth and diabetic retinopathy(4). Vascular endothelial growth factor (VEGF-A), a potent stimulator of angiogenesis, promotes endothelial cell proliferation, migration and tube formation(5), and also induces vascular permeability and inflammation(6).

Previous studies have demonstrated the increased glomerular filtration surface in diabetic nephropathy resulting from the formation of new glomerular capillaries and a slight elongation of the pre-existing capillaries(7; 8), analogous to the changes in pathologic diabetic retinopathy.

The increase in the levels of VEGF-A and the receptor of VEGF-A, VEGFR2 has been reported in diabetic nephropathy models(9; 10). In addition, the therapeutic efficacies of anti-VEGF-A strategies (i.e. neutralizing antibodies and a receptor tyrosine kinase inhibitor) have further demonstrated the involvement of VEGF-A in the progression of diabetic nephropathy(11-13).

The therapeutic effects of anti-angiogenic reagents, tumstatin peptide, endostatin peptide, angiostatin, pigment epithelium derived factor (PEDF) and NM-3(14-18) in diabetic nephropathy models have been reported by others and us.

Vasohibin-1 (VASH-1), an endogenous angiogenesis inhibitor, was identified from a microarray analysis to investigate genes up-regulated by VEGF in endothelial cells(19). The therapeutic effects of VASH-1 on tumor growth, atherosclerosis and proliferative retinopathy models have been reported(19-21). Based on the unique characteristics of this factor, VASH-1 is considered to act as an endothelial cell-derived negative feedback regulator of angiogenesis.

In the present study, we demonstrate the therapeutic efficacy of VASH-1 in ameliorating renal alterations in the streptozotocin (STZ)-induced mouse type 1 diabetes model. Treatment with adenoviral vector encoding human VASH-1 (AdhVASH-1) markedly suppressed characteristic alterations of early diabetic nephropathy. These effects were associated with the regulation of VEGFR2 activation in glomerular endothelial cells, and of TGF-β1, MCP-1 and receptor for AGE (RAGE) in mesangial cells.

RESEARCH DESIGN AND METHODS

Adenoviral vectors. A replication-defective adenoviral vector encoding human VASH-1 was prepared as previously described(19). A replication-defective adenovirus vector encoding the *Escherichia coli* β-galactosidase (AdLacZ), which is

identical to AdhVasohibin-1 (AdhVASH-1), except for the inserted cDNA, was used as the control(19) (see the online appendix available at http://diabetes.journals.org).

Induction of diabetes and experimental protocols. The experimental protocol was approved by the Animal Ethics Review Committee of Okayama University. Male ICR mice were fed a standard pellet laboratory chow and were provided with water *ad libitum*. Type 1 diabetes was induced by low-dose streptozotocin (STZ) injection as detailed by the NIDDK Consortium for Animal Models of Diabetic Complications'-(AMDCC) protocol (available from *http://www.amdcc.org*) with modification. Weight-matched 5-week-old male mice received intraperitoneal injections of streptozotocin (STZ, Sigma, St. Louis, MO; 120 mg/kg body weight) dissolved in 10 mM Sodium citrate, pH 5.5. Control mice received injections with buffer alone. STZ or citrate buffer was administered at three time points occurring at 48-hr intervals during the first week. Six days after the third injection of STZ, mice with blood glucose in the range of 13.9-22.2 mmol/l were divided into four subgroups: 1) non-diabetic control, diabetic mice treated with either 2) vehicle buffer (saline), 3) AdLacZ, or 4) AdhVASH-1 (n=5 for each subgroup). Thirty-two mice received injections of STZ and 15 mice exhibiting hyperglycemia in the range as described above were selected for experiments. At this point, intravenous injections of adenoviral vectors (AdLacZ or AdhVASH-1) or saline (via tail veins) were initiated using a syringe with a 27-gauge needle and were repeated every other week (5×10^9 vp/100 μl). Four weeks following the initial injections of adenoviral vectors (6 weeks after the induction of diabetes), mice were sacrificed and the kidneys were obtained.

No mice died and no signs of apparent exhaustion were observed during the experimental period (online appendix).

Blood and urine examination. Blood glucose was measured in tail-vein blood, and urine was tested for keton bodies and glucose by the OML, Inc. (Okayama Medical Laboratories, Okayama, Japan). Serum and urinary creatinine levels and urinary albumin concentration were determined as previously described(14). Results were normalized to the urinary creatinine levels, and expressed as the urinary albumin/creatinine ratio (UACR). The creatinine clearance (Ccr) was calculated and expressed as milliliters per minute per 100 g of body weight (online appendix).

Histological analysis. At 4 wks after starting treatment, kidneys were removed, fixed in 10% buffered formalin and embedded in paraffin. Sections (3-μm) were stained with periodic acid-Schiff (PAS) for light microscopic observation (online appendix).

Immunohistochemistry.Immunohistochemistry was performed using frozen sections as previously described(18; 22-24) (online appendix).

RNA extraction and quantitative real-time polymerase chain reaction (real-time PCR). RNA extraction and real-time PCR were performed as previously described with modifications(14; 18) (online appendix).

Immunoblot assay. Immunoblot assay was performed as previously described(18; 25) (online appendix).

***Recombinant* VASH-1.** Recombinant VASH-1 was prepared as previously described(19). Human vasohibin-1 protein connected to the FLAG tag at the C-terminus was expressed in a Bac-to-Bac baculovirus expression system (Invitrogen Corp) according to the manufacturer's instructions and purified as a soluble protein(19).

Cell culture. Primary murine mesangial cells (MES13) were utilized to determine the direct effect of recombinant human vasohibin-1 on high glucose-induced increase of the protein levels of VEGF, TGF-β, MCP-1 and RAGE as previously described(18; 26) (online appendix). Primary

human Glomerular microvascular Endothelial Cells (hGECs) were utilized to determine the direct effect of recombinant human VASH-1 on VEGF (R&D systems) or high glucose-induced increase of the phosphorylation of VEGFR2 (online appendix).

Statistical analysis. All values are expressed as mean +/- SEM. A Kruskal-Wallis test with *post-hoc* comparisons using the Scheffe's test was employed for inter-group comparisons of multiple variables. Statistical analysis was performed by SPSS Software for Windows (version 13.0, Chicago, IL). A level of $P < 0.05$ was considered statistically significant.

RESULTS

Serum and hepatic levels of VASH-1 following adenoviral transfer. The serum levels of VASH-1 were at very low levels in the non-diabetic mice (immunoblot). The AdhVASH-1-injected diabetic mice exhibited significantly elevated serum VASH-1 levels compared to the AdLacZ injection at 4 weeks after the initial injections (**Figure 1A).** Similarly, hepatic expression of VASH-1 was markedly elevated in the AdhVASH-1-injected diabetic mice **(Figure 1A).** The mice receiving AdLacZ or AdhVASH-1 did not exhibit any deleterious side effects and all the mice survived.

Non-diabetic male ICR mice receiving AdhVASH-1 did not exhibit any inflammatory or pathological alterations in the lungs, livers or kidneys (data not shown), and hypertension or proteinuria was not observed.

Changes in blood glucose, body weight (BW) and kidney weight/body weight (KW/BW). Treatment with AdhVASH-1 did not exhibit therapeutic effects on hyperglycemia **(Table 1)**. Body weight was significantly lower in all of the diabetic groups compared to non-diabetic animals, and AdhVASH-1 treatment did not significantly influence BW. Diabetic animals exhibited a significantly greater KW/BW ratio compared to non-diabetic mice **(Figure 1B)**. Injection of AdhVASH-1 resulted in a significantly decreased KW/BW ratio compared to the control diabetic mice **(Figure 1B)**.

Changes in blood pressure. There were no significant differences in blood pressure among non-diabetic animals, diabetic mice and diabetic mice treated with adenoviral vectors **(Table 1).**

Changes in serum creatinine, creatinine clearance (Ccr) and urinary albumin excretion. Serum creatinine levels did not significantly differ among the experimental groups. Although control diabetic mice showed a marked elevation of the Ccr and urinary albumin/creatinine ratio (UACR), AdhVASH-1 suppressed STZ-induced increase of Ccr and UACR **(Figure 1C and 1D**).

Histology and morphometric analysis. Glomerular hypertrophy and mesangial matrix expansion were significantly inhibited by AdhVASH-1 compared with the control diabetic animals **(Figure 1E-1H).** Morphometric analysis **(Figure 1I and 1J)** further confirmed the inhibitory effects of AdhVASH-1 on these parameters.

Immunohistochemical analysis of CD31(+) endothelial area. We next evaluated differences in the amount of the CD31(+) glomerular endothelial area by immunofluorescence staining. In non-diabetic mice, CD31 was detected in glomerular capillaries **(Figure 2A)**, and increase of the CD31(+) area in glomeruli was observed in control diabetic mice **(Figure 2B and 2C)**. Treatment with AdhVASH-1 markedly suppressed the increase of the glomerular CD31(+) area **(Figure 2D)**. Quantitative analysis **(Figure 2E)** further confirmed that the STZ-induced increase in the glomerular capillary area was significantly suppressed by AdhVASH-1. We also evaluated the $CD31^+$ peritubular capillary

(PTC) endothelial area to determine the potential adverse effects of VASH-1 on the survival of PTC. In the control diabetic mice, a slight increase of PTC density was observed, and AdhVASH-1 did not significantly influence the PTC density (**Online Appendix Figure 1**).

Protein levels of VEGF-A and receptor** VEGFR2 **in renal cortex. The effect of AdhVASH-1 on the expression of pro-angiogenic factor VEGF-A and corresponding receptors VEGFR2 in the renal cortex was studied by immunoblot assay. The level of VEGF-A and VEGFR2 was significantly increased in the control diabetic mice, which is consistent with previous reports (9; 15). Treatment with AdhVASH-1 did not affect the STZ-induced increase of VEGF-A, but significantly suppressed the increase of VEGFR2 compared with AdLacZ **(Figure 2F, 2G and 2H)**.

Phosphorylation of VEGFR2 in vivo and in cultured human glomerular microvascular endothelial cells. Next, we examined the potential inhibitory effects of VASH-1 on phosphorylation of VEGFR2. The ratio of phosphorylated VEGFR2 relative to total VEGFR2 in renal cortex of control diabetic mice was elevated compared to non-diabetic animals, and AdVASH-1 treatment showed inhibitory effects (**Figure 2G and 2I**). We next performed cell culture analysis using human glomerular microvascular endothelial cells (hGECs). The ratio of phosphorylated VEGFR2 relative to total VEGFR2 in hGECs was significantly increased at 2-15min after initiating stimulation with 10 nM VEGF as compared to control as detected by immunoblots (**Figure 3A**). Since the peak of pVEGFR2/VEGFR2 ratio was observed at 5 min after stimulation with VEGF, we performed following experiments under this condition. Increase in the levels of pVEGFR2/VEGFR2 ratio was significantly suppressed by recombinant VASH-1 as detected by immunoblots (**Figure 3B**). Similarly, the levels of pVEGFR2/VEGFR2 ratio in hGECs was significantly increased at 24 hour after incubation in medium supplemented with 25 mM glucose (high glucose; HG) as compared to incubation under the normal glucose condition (normal glucose; NG) as detected by immunoblots (**Figure 3C**). Addition of mannitol to the culture condition under normal glucose did not lead to the significant increase of pVEGFR2/VEGFR2 ratio, thus excluding the potential effect caused by elevated osmotic pressure. Treatment with recombinant VASH-1 resulted in the suppression of the increase of pVEGFR2/VEGFR2 ratio induced by high glucose in a dose-dependent manner (**Figure 3C**).

Immunohistochemical analysis of glomerular type IV collagen. Next, the accumulation of glomerular type IV collagen was examined by immunofluorescence staining **(Figure 4)**. The amount of type IV collagen in glomeruli was increased in the control diabetic group **(Figure 4B and 4C)** as compared to the non-diabetic mice **(Figure 4A)**. Enhanced immunoreactivity in the diabetic mice was observed mainly in the glomerular basement membrane and mesangial area. Treatment with AdhVASH-1 decreased the accumulation of type IV collagen induced by STZ compared with AdLacZ treatment **(Figure 4D)** and these results were further confirmed by quantitative morphometric analysis **(Figure 4G)**.

Immunohistochemical analysis of monocyte/macrophage infiltration. We next examined glomerular infiltration of monocytes/macrophages by immunohistochemistry for F4/80. In the control diabetic mice, the number of F4/80(+) cells was significantly increased as compared to the non-diabetic mice. Treatment with AdhVASH-1 markedly decreased the accumulation of monocytes/macrophages in glomeruli **(Figure 4H)**.

Protein and mRNA levels of TGF-β1 in renal cortex. TGF-β1 is a pro-fibrotic factor involved in mesangial matrix expansion and renal hypertrophy in diabetic nephropathy(27). The control diabetic mice exhibited increased levels of TGF-β protein compared with the non-diabetic animals in the renal cortex (immunoblots). AdhVASH-1 significantly suppressed the increase of TGF-β in the diabetic animals compared with AdLacZ **(Figure 5A and 5B)**. Similarly, inhibitory effects of AdhVASH-1 on the levels of TGF-β1 mRNA were observed by real-time PCR **(Figure 5C)**.

Protein and mRNA levels of MCP-1 in renal cortex. MCP-1 is one of the crucial chemokines involved in the development of diabetic nephropathy(28). Control diabetic mice exhibited increased levels of MCP-1 protein compared with non-diabetic animals in the renal cortex (immunoblot). Treatment with AdhVASH-1 resulted in the suppression of MCP-1 protein levels compared with AdLacZ **(Figure 5D and 5E)**. Similar inhibitory effects of AdhVASH-1 on the increase of the mRNA levels of MCP-1 in diabetic animals were observed **(Figure 5F)**.

Protein levels of RAGE in renal cortex. The potential role of advanced glycation end products (AGE) in the pathogenesis of diabetic nephropathy has been reported(29). Receptor for AGE (RAGE), a well-characterized cell surface receptor for AGE, plays an important role in the development of diabetic nephropathy(30). The control diabetic mice exhibited increased protein levels of RAGE compared with non-diabetic animals in the renal cortex (immunoblots). Treatment with AdhVASH-1 resulted in the suppression of RAGE protein levels compared with AdLacZ treatment **(Figure 5G and 5H)**.

Protein levels of TGF-β, MCP-1 and RAGE in cultured mouse mesangial cells. To examine the potential direct effects of VASH-1 on non-endothelial cells in association with the observed therapeutic effects *in vivo*, we performed cell culture analysis using primary mouse mesangial cells. The protein level of TGF-β, MCP-1 and RAGE in mesangial cells was significantly increased at 48 hours after incubation in HG condition as compared to incubation under NG condition as detected by immunoblots (**Figure 6**). Addition of mannitol to the NG condition did not lead to the increase of TGF-β, MCP-1 and RAGE, thus excluding the potential effect by elevated osmotic pressure. Treatment with recombinant VASH-1 resulted in the suppression of the increase of protein levels for TGF-β, MCP-1 and RAGE induced by HG in a dose-dependent manner (**Figure 6**).

Localization and the levels of endogenous mouse VASH-1 in kidney. In non-diabetic mice, endogenous mouse VASH-1 (mVASH-1) was observed in arterioles and in glomeruli. Immunoreactivity for mVASH-1 was increased in diabetic glomeruli, and was remarkable in the mesangial (α-SMA$^+$) area and also in endothelial (CD31$^+$) area as detected by double immunofluorescent staining (**Figure 7A and 7B**). In blood vessels, mVASH-1 was mainly localized to the outer aspect of vessels, presumably in smooth muscle cells (α-SMA$^+$) and in the adventitia, and slightly observed in the endothelium (CD31$^+$) as well (**Figure 7A and 7B**). Immunoblot analysis revealed a mild increase of renal endogenous mVASH-1 in the vehicle-treated diabetic mice compared to the non-diabetic control mice without statistically significant difference **(Online Appendix Figure 2)**. Treatment with AdhVASH-1 did not alter the levels of endogenous mVASH-1 compared to the control diabetic mice.

DISCUSSION

In the present study, we utilized a streptozotocin-induced type 1 diabetes mouse model to demonstrate the therapeutic efficacy of vasohibin-1. Although renal failure is not easily reproducible, some of the characteristic early alterations in human diabetic nephropathy such as albuminuria, glomerular hyperfiltration and some of the characteristic histopathologic changes can be observed in this model(31). Intravenous administration of AdhVASH-1 resulted in the sustained increase of serum levels of hVASH-1 presumably derived from liver, without causing any systemic inflammatory reactions. Additionally, administration of AdhVASH-1 in non-diabetic mice did not cause any inflammatory histological alterations in the kidney. Therefore, we consider the present approach employing adenoviral vectors as non-harmful for experimental animals. Treatment with AdhVASH-1 did not affect hyperglycemia or body weight loss induced by STZ, similar to our previous observations using anti-angiogenic tumstatin peptide and endostatin peptide(14; 15). Although diabetic mice exhibited significant weight loss, the extent of reduced body weight was comparable to previous reports utilizing this model. In the control diabetic mice, characteristic alterations in early diabetic nephropathy such as albuminuria, glomerular hypertrophy, glomerular hyperfiltration as evidenced by increased creatinine clearance (Ccr), and renal hypertrophy were observed. These early abnormalities in diabetic nephropathy were significantly inhibited by AdhVASH-1 compared with AdLacZ treatment. Histological assessment demonstrated that treatment with AdhVASH-1 suppressed the increase of the CD31(+) glomerular endothelial area in diabetic mice. Experimental diabetic animals exhibit an increased glomerular filtration surface area as well as glomerular capillary number in the early stage of the disease(7; 8). AdhVASH-1 treatment has suppressed these alterations potentially via the anti-angiogenic efficacy, leading to the observed therapeutic effects on the increase of Ccr and albuminuria.

In the present study, the level of VEGF-A was increased in the renal cortex of diabetic mice, consistent with previous studies(9; 10; 14). Recent reports have demonstrated reduced expression of VEGF-A in human diabetic nephropathy patients(32; 33). Although diabetic animal models are often studied in a relatively early phase of the disease, most diabetic patients employed in clinical studies were already in a moderately advanced stage. For instance, reduced VEGF expression in the renal interstitium was associated with interstitial vascular rarefaction in a study using samples of human diabetic nephropathy(33), but we could not detect a reduction of PTC density in the present study in the control diabetic animals. Treatment with AdhVASH-1 did not diminish the increase of VEGF-A in the renal cortex, but resulted in the suppression of the increase of VEGFR2. The regulatory role of VASH-1 on VEGFR2, but not VEGF-A is consistent with previous results on proliferative retinopathy(21). In addition, VASH-1 significantly suppressed the increase of pVEGFR2/VEGFR2 ratio in diabetic animals as well as in cultured glomerular endothelial cells. Our results are not consistent with previous reports demonstrating that VASH-1 did not inhibit VEGF-induced VEGFR2 phosphorylation in HUVECs(19). Unique characteristics of the glomerular endothelial cells possessing fenestration are well known, and such differences among distinct endothelial cell-types may underlie the discrepant response to VASH-1 in regard to VEGFR-2 phosphorylation. The therapeutic effect of VASH-1 in early diabetic nephropathy, at least in part, may be attributed to the inhibition of overactivation of the VEGF-A pathway in analogy with previous studies utilizing neutralizing anti-VEGF-A antibodies(11; 12) and a recent

report demonstrating that inducible overexpression of soluble flt-1 (VEGFR1), an antagonist of VEGF-A, in podocytes ameliorated diabetic glomerular alterations in mice(34). To date, cell surface receptors for VASH-1 as well as potential influence of VASH-1 on intracellular signal transduction have not been fully identified, and future analysis on crosstalk between VASH-1 signaling and VEGF signaling is required.

We observed a significant inhibitory effect of AdhVASH-1 on renal hypertrophy in diabetic mice. VEGF-A augments protein synthesis and hypertrophy in renal proximal tubular epithelial cells(35). Considering the dominant contribution of the tubular compartment in organizing renal mass, we speculate that AdhVASH-1 might have affected the tubular hypertrophy potentially via regulating VEGF-A-mediated signaling.

In the present study, increase in the levels of renal TGF-β was significantly suppressed by AdhVASH-1, potentially associated with therapeutic efficacy on the accumulation of ECM. These results are consistent with previous reports demonstrating the inhibitory effects of anti-angiogenic reagents on ECM accumulation in animal models of diabetic nephropathy(14-16; 18; 36).

Interestingly, recombinant VASH-1 treatment resulted in the suppression of the increase of TGF-β induced by HG in cultured mesangial cells. We previously observed similar inhibitory effects of NM-3 on high glucose-induced TGF-β production in mesangial cells(18), suggesting the novel potential therapeutic mechanisms of anti-angiogenic factors mediated via direct interaction with 'non-endothelial' mesangial cells.

A recent report has demonstrated the potential role of VEGF in mediating glomerular monocyte/macrophage infiltration in a diabetic animal model(37). Therefore, observed anti-inflammatory effect of VASH-1 might be, at least in part, associated with regulation of vascular permeability. Yamashita *et al*. have demonstrated the therapeutic role of AdhVASH-1 in preventing arterial neointimal formation(20). Adventitial macrophage infiltration were inhibited by AdhVASH-1(20), similar to our present results. In addition, VASH-1 suppressed renal MCP-1 expression in diabetic animals, and suppressed the increase of MCP-1 induced by HG in cultured mesangial cells. The inhibitory effect of AdhVASH-1 on the increase of chemokines may also mediate its anti-inflammatory effects. Previous reports have demonstrated the association between infiltration of macrophages and the accumulation of ECM proteins in the mesangium in diabetic models(38; 39). Regarding the source of TGF-β, macrophages as well as mesangial cells can secrete TGF-β(40). Thus, we speculate that the observed regulatory effects of VASH-1 on the accumulation of monocytes/ macrophages might have contributed to the inhibition of mesangial matrix accumulation.

The deleterious effects of AGE in the development of diabetic nephropathy, and the therapeutic effects of AGE inhibitors in preventing the progression of experimental diabetic nephropathy were previously reported(10; 41). AGE induces overexpression of TGF-β, MCP-1 and VEGF in cultured mesangial cells(42; 43). Interaction of AGE with RAGE plays an important role in diabetic nephropathy(44). VASH-1 significantly suppressed renal RAGE levels in diabetic mice, and suppressed the increase of RAGE induced by HG in cultured mesangial cells. These results suggest that anti-fibrotic and anti-inflammatory effects of VASH-1 were partially mediated via down-regulating RAGE levels in mesangial cells resulting in the suppression of TGF-β and MCP-1.

Regarding endogenous levels and localization of mouse VASH-1 (mVASH-1), renal protein levels of mVASH-1 were mildly

increased in diabetic control mice. AdhVASH-1 did not alter renal mVASH-1 levels compared with AdLacZ treatment. In diabetic mice, mVASH-1 was observed in the glomerular endothelium and mesangial area. Previous reports have revealed the localization of human VASH-1 in endothelium of the placenta, endometria, brain, atherosclerotic lesions and choroidal neovascular membranes(19; 20; 45; 46). Mouse VASH-1 was expressed in the retinal endothelial cells in mice with ischemic retinopathy(21). The localization of mVASH-1 in the mesangial area suggests the synthesis of VASH-1 in mesangial cells, but also the potential mesangial deposition of VASH-1 released from endothelial cells could not be excluded. Studies using VASH-1-deficient mice(47) may clarify biological roles of endogenous mVASH-1 in diabetic nephropathy in future.

There are several limitations to the present study. Systemic administration of anti-angiogenic reagents may lead to reduced angiogenic response in a setting requiring neovessel formation such as myocardial infarction and limb ischemia; pathological conditions complicated in advanced diabetic patients. Neointimal formation is the crucial cause of luminal narrowing of arteries in atherosclerosis. Although further assessment in the advanced stage is required, AdhVASH-1 might be tolerable or even therapeutic for atherosclerotic conditions considering a previous report showing the therapeutic effects of AdhVASH-1 in preventing neointimal formation(20). The crucial involvement of chronic hypoxia in association with reduction of peritubular capillaries (PTC) in progressing tubulointertstitial injuries has been reported(48). AdhVASH-1 did not reduce PTC density in the present model, suggesting its safety in diabetic nephropathy. However, careful evaluation on the potential influence of VASH-1 on PTC density in advanced diabetic nephropathy might be required.

Considering application to diabetic patients, potential adverse events accompanied by the injection of adenoviral vectors such as non-specific inflammatory reactions and the replication of adenoviruses *in vivo* should be avoided, and further assessments on the safety of this strategy are required.

Recently, Eremina *et al.* have demonstrated the potential adverse events of bevacizumab, a humanized monoclonal antibody against VEGF, resulting in thrombotic microangiopathy in patients with cancer(49). Considering the lack of such histological alterations in previous experimental studies employing anti-VEGF antibodies or SU5416(11-13), anti-VEGF therapy might not be detrimental for patients with diabetic nephropathy. More recently, Ku *et al*. have demonstrated that inducible podocyte-specific overexpression of sVEGFR1 in adult mice ameliorated diabetic glomerular alterations(34), suggesting the involvement of VEGF-A in diabetic nephropathy. Although VASH-1 suppresses overactivation of VEGFR2, it does not serve as a specific inhibitor of VEGF signaling(19). In addition, AdhVASH-1 did not cause proteinuria in non-diabetic mice. Thus, VASH-1 treatment is distinct from strategies with specific inhibition of VEGF, potentially associated with less adverse events.

In conclusion, we demonstrated that VASH-1 effectively ameliorated alterations in an animal model of early diabetic nephropathy. Our results demonstrate the direct effects of VASH-1 on glomerular endothelial and mesangial cells in association with anti-angiogenic, anti-fibrotic and anti-inflammatory mechanisms and regulatory effects on RAGE-mediated pathways. We believe that our present study will eventually guide us to the development of novel

therapeutic strategies for patients with diabetic nephropathy.

ACKNOWLEDGMENTS

A portion of this study was supported by a research grant from a Grant-in-Aid for Scientific Research from the Ministry of Education, Science and Culture of Japan (2005-2009, YM), Grant-in-Aid from the Japan Diabetes Foundation (2005, YM), the Takeda Science Foundation (2006, YM) and the Japan Foundation of Cardiovascular Research (2006, YM).

A portion of this work was published in abstract form (*J Am Soc Nephrol* 18:654A, 2007).

We are grateful to appreciate Dr. Toshiyoshi Fujiwara (Center for Gene and Cell Therapy, Okayama Univ. Hospital) for his technical assistance in preparing adenoviral vectors and Dr. Kei Sarai (Department of Medicine and Clinical Science, Okayama University Graduate School of Medicine, Dentistry and Pharmaceutical Sciences) for his technical assistance in cell culture of glomerular endothelial cells.

Table 1. Body weight, blood glucose concentration and blood pressure.

Group	Body weight (g)	Blood glucose (mmol/l)	MBP (mmHg)
Non-diabetic	35.8 ± 0.2	7.3 ± 0.3	80.6 ± 3.0
Diabetic (vehicle)	30.8 ± 1.8*	27.3 ± 0.7*	80.9 ± 1.7
Diabetic (Ad-LacZ)	31.6 ± 2.1*	27.6 ± 1.2*	78.9 ± 2.6
Diabetic (Ad-VASH1)	30.6 ± 0.6*	27.8 ± 0.9*	80.3 ± 2.0

*$P < 0.05$ *vs.* non-diabetic animals. Values are shown as mean ± SEM. N = 5 in each group. Vehicle; vehicle buffer-treated, VASH-1; Vasohibin-1. MBP: mean blood pressure.

REFERENCES

1. Makino H, Kashihara N, Sugiyama H, Kanao K, Sekikawa T, Okamoto K, Maeshima Y, Ota Z, Nagai R: Phenotypic modulation of the mesangium reflected by contractile proteins in diabetes. *Diabetes* 45:488-495., 1996
2. Sharma K, Ziyadeh FN: Hyperglycemia and diabetic kidney disease. The case for transforming growth factor-beta as a key mediator. *Diabetes* 44:1139-1146, 1995
3. Brownlee M, Cerami A, Vlassara H: Advanced glycosylation end products in tissue and the biochemical basis of diabetic complications. *N Engl J Med* 318:1315-1321, 1988
4. Folkman J: Angiogenesis in cancer, vascular, rheumatoid and other disease. *Nat Med* 1:27-31, 1995
5. Ferrara N: Vascular endothelial growth factor and the regulation of angiogenesis. *Recent Prog Horm Res* 55:15-35, 2000
6. Dvorak HF, Brown LF, Detmar M, Dvorak AM: Vascular permeability factor/vascular endothelial growth factor, microvascular hyperpermeability, and angiogenesis. *Am J Pathol* 146:1029-1039, 1995
7. Nyengaard JR, Rasch R: The impact of experimental diabetes mellitus in rats on glomerular capillary number and sizes. *Diabetologia* 36:189-194, 1993
8. Guo M, Ricardo SD, Deane JA, Shi M, Cullen-McEwen L, Bertram JF: A stereological study of the renal glomerular vasculature in the db/db mouse model of diabetic nephropathy. *J Anat* 207:813-821, 2005
9. Cooper ME, Vranes D, Youssef S, Stacker SA, Cox AJ, Rizkalla B, Casley DJ, Bach LA, Kelly DJ, Gilbert RE: Increased renal expression of vascular endothelial growth factor (VEGF) and its receptor VEGFR-2 in experimental diabetes. *Diabetes* 48:2229-2239, 1999
10. Tsuchida K, Makita Z, Yamagishi S, Atsumi T, Miyoshi H, Obara S, Ishida M, Ishikawa S, Yasumura K, Koike T: Suppression of transforming growth factor beta and vascular endothelial growth factor in diabetic nephropathy in rats by a novel advanced glycation end product inhibitor, OPB-9195. *Diabetologia* 42:579-588., 1999
11. de Vriese AS, Tilton RG, Elger M, Stephan CC, Kriz W, Lameire NH: Antibodies against vascular endothelial growth factor improve early renal dysfunction in experimental diabetes. *J Am Soc Nephrol* 12:993-1000, 2001
12. Flyvbjerg A, Dagnaes-Hansen F, De Vriese AS, Schrijvers BF, Tilton RG, Rasch R: Amelioration of long-term renal changes in obese type 2 diabetic mice by a neutralizing vascular endothelial growth factor antibody. *Diabetes* 51:3090-3094, 2002
13. Sung SH, Ziyadeh FN, Wang A, Pyagay PE, Kanwar YS, Chen S: Blockade of vascular endothelial growth factor signaling ameliorates diabetic albuminuria in mice. *J Am Soc Nephrol* 17:3093-3104, 2006
14. Yamamoto Y, Maeshima Y, Kitayama H, Kitamura S, Takazawa Y, Sugiyama H, Yamasaki Y, Makino H: Tumstatin Peptide, an inhibitor of angiogenesis, prevents glomerular hypertrophy in the early stage of diabetic nephropathy. *Diabetes* 53:1831-1840, 2004
15. Ichinose K, Maeshima Y, Yamamoto Y, Kitayama H, Takazawa Y, Hirokoshi K, Sugiyama H, Yamasaki Y, Eguchi K, Makino H: Anti-angiogenic endostatin peptide ameliorates renal alterations in the early stage of type 1 diabetic nephropathy model. *Diabetes* 54:2891-2903, 2005
16. Zhang SX, Wang JJ, Lu K, Mott R, Longeras R, Ma JX: Therapeutic potential of angiostatin in diabetic nephropathy. *J Am Soc Nephrol* 17:475-486, 2006

17. Wang JJ, Zhang SX, Mott R, Chen Y, Knapp RR, Cao W, Ma JX: Anti-inflammatory effects of pigment epithelium-derived factor in diabetic nephropathy. *Am J Physiol Renal Physiol* 294:F1166-1173, 2008
18. Ichinose K, Maeshima Y, Yamamoto Y, Kinomura M, Hirokoshi K, Kitayama H, Takazawa Y, Sugiyama H, Yamasaki Y, Agata N, Makino H: 2-(8-hydroxy-6-methoxy-1-oxo-1h-2-benzopyran-3-yl) propionic acid, an inhibitor of angiogenesis, ameliorates renal alterations in obese type 2 diabetic mice. *Diabetes* 55:1232-1242, 2006
19. Watanabe K, Hasegawa Y, Yamashita H, Shimizu K, Ding Y, Abe M, Ohta H, Imagawa K, Hojo K, Maki H, Sonoda H, Sato Y: Vasohibin as an endothelium-derived negative feedback regulator of angiogenesis. *J Clin Invest* 114:898-907, 2004
20. Yamashita H, Abe M, Watanabe K, Shimizu K, Moriya T, Sato A, Satomi S, Ohta H, Sonoda H, Sato Y: Vasohibin prevents arterial neointimal formation through angiogenesis inhibition. *Biochem Biophys Res Commun* 345:919-925, 2006
21. Shen J, Yang X, Xiao WH, Hackett SF, Sato Y, Campochiaro PA: Vasohibin is up-regulated by VEGF in the retina and suppresses VEGF receptor 2 and retinal neovascularization. *Faseb J* 20:723-725, 2006
22. Maeshima Y, Kashihara N, Yasuda T, Sugiyama H, Sekikawa T, Okamoto K, Kanao K, Watanabe Y, Kanwar YS, Makino H: Inhibition of mesangial cell proliferation by E2F decoy oligodeoxynucleotide in vitro and in vivo. *J Clin Invest* 101:2589-2597., 1998
23. Tanabe K, Maeshima Y, Ichinose K, Kitayama H, Takazawa Y, Hirokoshi K, Kinomura M, Sugiyama H, Makino H: Endostatin peptide, an inhibitor of angiogenesis, prevents the progression of peritoneal sclerosis in a mouse experimental model. *Kidney Int* 71:227-238, 2007
24. Kinomura M, Kitamura S, Tanabe K, Ichinose K, Hirokoshi K, Takazawa Y, Kitayama H, Nasu T, Sugiyama H, Yamasaki Y, Sugaya T, Maeshima Y, Makino H: Amelioration of cisplatin-induced acute renal injury by renal progenitor-like cells derived from the adult rat kidney. *Cell Transplant* 17:143-158, 2008
25. Maeshima Y, Sudhakar A, Lively JC, Ueki K, Kharbanda S, Kahn CR, Sonenberg N, Hynes RO, Kalluri R: Tumstatin, an endothelial cell-specific inhibitor of protein synthesis. *Science* 295:140-143., 2002
26. Baba M, Wada J, Eguchi J, Hashimoto I, Okada T, Yasuhara A, Shikata K, Kanwar YS, Makino H: Galectin-9 inhibits glomerular hypertrophy in db/db diabetic mice via cell-cycle-dependent mechanisms. *J Am Soc Nephrol* 16:3222-3234, 2005
27. Sharma K, Jin Y, Guo J, Ziyadeh FN: Neutralization of TGF-beta by anti-TGF-beta antibody attenuates kidney hypertrophy and the enhanced extracellular matrix gene expression in STZ-induced diabetic mice. *Diabetes* 45:522-530, 1996
28. Wada T, Furuichi K, Sakai N, Iwata Y, Yoshimoto K, Shimizu M, Takeda SI, Takasawa K, Yoshimura M, Kida H, Kobayashi KI, Mukaida N, Naito T, Matsushima K, Yokoyama H: Up-regulation of monocyte chemoattractant protein-1 in tubulointerstitial lesions of human diabetic nephropathy. *Kidney Int* 58:1492-1499, 2000
29. Vlassara H, Striker LJ, Teichberg S, Fuh H, Li YM, Steffes M: Advanced glycation end products induce glomerular sclerosis and albuminuria in normal rats. *Proc Natl Acad Sci U S A* 91:11704-11708, 1994
30. Yamamoto Y, Kato I, Doi T, Yonekura H, Ohashi S, Takeuchi M, Watanabe T, Yamagishi S, Sakurai S, Takasawa S, Okamoto H, Yamamoto H: Development and prevention of advanced diabetic nephropathy in RAGE-overexpressing mice. *J Clin Invest* 108:261-268, 2001

31. Breyer MD, Bottinger E, Brosius FC, 3rd, Coffman TM, Harris RC, Heilig CW, Sharma K: Mouse models of diabetic nephropathy. *J Am Soc Nephrol* 16:27-45, 2005
32. Baelde HJ, Eikmans M, Lappin DW, Doran PP, Hohenadel D, Brinkkoetter PT, van der Woude FJ, Waldherr R, Rabelink TJ, de Heer E, Bruijn JA: Reduction of VEGF-A and CTGF expression in diabetic nephropathy is associated with podocyte loss. *Kidney Int* 71:637-645, 2007
33. Lindenmeyer MT, Kretzler M, Boucherot A, Berra S, Yasuda Y, Henger A, Eichinger F, Gaiser S, Schmid H, Rastaldi MP, Schrier RW, Schlondorff D, Cohen CD: Interstitial vascular rarefaction and reduced VEGF-A expression in human diabetic nephropathy. *J Am Soc Nephrol* 18:1765-1776, 2007
34. Ku CH, White KE, Dei Cas A, Hayward A, Webster Z, Bilous R, Marshall S, Viberti G, Gnudi L: Inducible overexpression of sFlt-1 in podocytes ameliorates glomerulopathy in diabetic mice. *Diabetes* 57:2824-2833, 2008
35. Senthil D, Choudhury GG, McLaurin C, Kasinath BS: Vascular endothelial growth factor induces protein synthesis in renal epithelial cells: a potential role in diabetic nephropathy. *Kidney Int* 64:468-479, 2003
36. Wang JJ, Zhang SX, Mott R, Knapp RR, Cao W, Lau K, Ma JX: Salutary effect of pigment epithelium-derived factor in diabetic nephropathy: evidence for antifibrogenic activities. *Diabetes* 55:1678-1685, 2006
37. Sato W, Kosugi T, Zhang L, Roncal CA, Heinig M, Campbell-Thompson M, Yuzawa Y, Atkinson MA, Grant MB, Croker BP, Nakagawa T: The pivotal role of VEGF on glomerular macrophage infiltration in advanced diabetic nephropathy. *Lab Invest* 88:949-961, 2008
38. Sassy-Prigent C, Heudes D, Mandet C, Belair MF, Michel O, Perdereau B, Bariety J, Bruneval P: Early glomerular macrophage recruitment in streptozotocin-induced diabetic rats. *Diabetes* 49:466-475, 2000
39. Okada S, Shikata K, Matsuda M, Ogawa D, Usui H, Kido Y, Nagase R, Wada J, Shikata Y, Makino H: Intercellular adhesion molecule-1-deficient mice are resistant against renal injury after induction of diabetes. *Diabetes* 52:2586-2593, 2003
40. Leonarduzzi G, Scavazza A, Biasi F, Chiarpotto E, Camandola S, Vogel S, Dargel R, Poli G: The lipid peroxidation end product 4-hydroxy-2,3-nonenal up-regulates transforming growth factor beta1 expression in the macrophage lineage: a link between oxidative injury and fibrosclerosis. *Faseb J* 11:851-857, 1997
41. Soulis-Liparota T, Cooper M, Papazoglou D, Clarke B, Jerums G: Retardation by aminoguanidine of development of albuminuria, mesangial expansion, and tissue fluorescence in streptozocin-induced diabetic rat. *Diabetes* 40:1328-1334, 1991
42. Yamagishi S, Inagaki Y, Okamoto T, Amano S, Koga K, Takeuchi M, Makita Z: Advanced glycation end product-induced apoptosis and overexpression of vascular endothelial growth factor and monocyte chemoattractant protein-1 in human-cultured mesangial cells. *J Biol Chem* 277:20309-20315, 2002
43. Fukami K, Ueda S, Yamagishi S, Kato S, Inagaki Y, Takeuchi M, Motomiya Y, Bucala R, Iida S, Tamaki K, Imaizumi T, Cooper ME, Okuda S: AGEs activate mesangial TGF-beta-Smad signaling via an angiotensin II type I receptor interaction. *Kidney Int* 66:2137-2147, 2004
44. Yamamoto Y, Doi T, Kato I, Shinohara H, Sakurai S, Yonekura H, Watanabe T, Myint KM, Harashima A, Takeuchi M, Takasawa S, Okamoto H, Hashimoto N, Asano M, Yamamoto H:

Receptor for advanced glycation end products is a promising target of diabetic nephropathy. *Ann N Y Acad Sci* 1043:562-566, 2005

45. Yoshinaga K, Ito K, Moriya T, Nagase S, Takano T, Niikura H, Yaegashi N, Sato Y: Expression of vasohibin as a novel endothelium-derived angiogenesis inhibitor in endometrial cancer. *Cancer Sci* 99:914-919, 2008
46. Wakusawa R, Abe T, Sato H, Yoshida M, Kunikata H, Sato Y, Nishida K: Expression of vasohibin, an antiangiogenic factor, in human choroidal neovascular membranes. *Am J Ophthalmol* 146:235-243, 2008
47. Kimura H, Miyashita H, Suzuki Y, Kobayashi M, Watanabe K, Sonoda H, Ohta H, Fujiwara T, Shimosegawa T, Sato Y: Distinctive localization and opposed roles of vasohibin-1 and vasohibin-2 in the regulation of angiogenesis. *Blood* 113:4810-4818, 2009 [Epub ahead of print]
48. Nangaku M: Chronic hypoxia and tubulointerstitial injury: a final common pathway to end-stage renal failure. *J Am Soc Nephrol* 17:17-25, 2006
49. Eremina V, Jefferson JA, Kowalewska J, Hochster H, Haas M, Weisstuch J, Richardson C, Kopp JB, Kabir MG, Backx PH, Gerber HP, Ferrara N, Barisoni L, Alpers CE, Quaggin SE: VEGF inhibition and renal thrombotic microangiopathy. *N Engl J Med* 358:1129-1136, 2008

Figure Legends

Fig. 1. *A*: Immunoblot analysis. Immunoblot for human VASH-1 and actin are shown. Each lane was loaded with 50 μg protein obtained from the serum samples or liver. The AdhVASH-1-injected diabetic mice exhibited significantly elevated serum VASH-1 (42 kD) levels compared to the AdLacZ-injected diabetic mice (4 weeks). Similarly, enhanced protein levels of VASH-1 in the liver were observed in AdhVASH-1-treated mice compared with AdLacZ-treated diabetic mice. Immunoblots for actin are shown to confirm equal loading. *B*: Increase in kidney weight-to-body weight ratio induced by STZ was diminished in the AdhVASH-1-treated diabetic group. Kidney weight relative to body weight was determined before termination of the experiments. *C*: Increase in UACR induced by STZ was significantly suppressed by treatment with AdhVASH-1. Data obtained at 4 weeks after initiating treatment with Ad-LacZ or AdhVASH-1 is shown. *D*: Increase in Ccr induced by STZ was partially suppressed by AdhVASH-1. *B-D*: $^{*}P < 0.05$ vs. N. $^{\dagger}P < 0.05$ vs. Ve or LacZ. *E-H*: Representative light microscopic appearance of glomeruli (periodic acid-Schiff staining, original magnification x400) for non-diabetic control mice (*E*), diabetic mice treated with either vehicle buffer (*F*), AdLacZ (*G*), or AdhVASH-1 (*H*). *I*: Increase in glomerular volume induced by STZ was diminished by treatment with AdhVASH-1. *J*: Mesangial matrix index was defined as the proportion of the glomerular tuft occupied by the mesangial matrix area (excluding nuclei). *I and J*: $^{*}P < 0.01$ vs. N. $^{\dagger}P < 0.01$ vs. Ve or LacZ. $n = 5$ for each group. N, non-diabetic control; Ve, diabetic mice treated with vehicle buffer; LacZ, diabetic mice treated with AdLacZ ($5x10^{9}$vp/mice); Vas, diabetic mice treated with AdhVASH-1 ($5x10^{9}$vp/mice). Each column consists of means ± SE.

Fig. 2. *A-E*: Immunofluorescent staining of CD31, an endothelial cell marker. Distribution of CD31 was determined by indirect immunofluorescence technique in non-diabetic control mice (*A*), diabetic mice treated with either vehicle buffer (*B*), AdLacZ (*C*), or AdhVASH-1 (*D*). *E*: Glomerular CD31(+) endothelial area was quantitated. Increase in the CD31(+) glomerular capillary area was significantly suppressed after treatment with AdhVASH-1. $^{*}P < 0.01$ vs. N. $^{\dagger}P < 0.01$ vs. Ve or LacZ. *F and G*: Immunoblot analysis. Immunoblots for VEGF-A, phosphorylated VEGFR2 (pVEGFR2), total VEGFR2 and actin are shown. Each lane was loaded with 50 μg protein obtained from the renal cortex. Each band was scanned and subjected to densitometry. *F (lower panels)*: Intensities of VEGF-A protein relative to actin are shown. $^{*}P < 0.01$ vs. N. *H and I*: Intensities of pVEGFR2 relative to total VEGFR2 (upper graph) and those of VEGFR2 relative to actin (lower graph) are shown. $^{*}P < 0.01$ vs. N. $^{\dagger}P < 0.05$ vs. Ve or LacZ. $n = 5$ for each group.

Fig. 3. *A-C*: Immunoblot analysis (cultured human glomerular microvascular endothelial cells, hGECs). Immunoblots for pVEGFR2, VEGFR2 and actin are shown. *A*: Cells were stimulated with 20 ng/mL of VEGF for 2-15 min. Intensities of pVEGFR2 protein relative to total VEGFR2 are shown. $*P < 0.01$ vs. control (0). *B*: Cells were stimulated with 20 ng/mL of VEGF for 5 min in the presence of recombinant VASH-1 (0-20 nM). Intensities of pVEGFR2 protein relative to VEGFR2 are shown. $*P < 0.01$ vs. control. $^{\dagger}P < 0.05$ vs. VEGF(+)/VASH-1(0). *C*: Cells were cultured under normal glucose (NG, 5.5 mM) or high glucose (HG, 25 mM) for 24 hrs in the presence of recombinant VASH-1 (0-20 nM). Intensities of pVEGFR2 protein relative to VEGFR2 are shown. $*P < 0.01$ vs. NG or NG/Manni. $^{\dagger}P < 0.05$ vs. HG/V0. Each lane was loaded with 15 μg protein obtained from

hGECs. NG+Manni, normal D-glucose plus D-mannitol (19.5 mmol/L); V0, without VASH-1; V1, 1 nM VASH-1**;** V10, 10 nM VASH-1**;** V20, 20 nM VASH-1.

Fig. 4. *A-D*: Glomerular accumulation of type IV collagen was assessed by the indirect immunofluorescence method for non-diabetic control mice (*A*), diabetic mice treated with either vehicle buffer (*B*), AdLacZ (*C*), or AdhVASH-1 (*D*). *A-D:* Original magnification x200. *E and F*: Immunohistochemistry of F4/80$^+$ monocyte/ macrophage. Representative light microscopic appearances of glomerulus in diabetic mice treated with vehicle buffer stained in the presence of the primary antibodies (*E*) or normal rat IgG (*F*) are shown. F4/80$^+$ cells were observed in diabetic mice (arrowheads; original magnification x400). *G*: The amount of immunoreactive type IV collagen in glomeruli relative to the non-diabetic control group determined by computer image analysis is shown. *H*: The number of glomerular F4/80$^+$ monocyte/macrophages is shown. Increase in the F4/80$^+$ monocyte/macrophage number was significantly suppressed after treatment with AdhVASH-1. $n = 5$ for each group. $^*P < 0.01$ vs. N. $^\dagger P < 0.01$ vs. Ve or LacZ.

Fig. 5. Immunoblot analysis and real-time PCR of TGF-β, MCP-1 and RAGE. *A, D and G*: Immunoblots for TGF-β, MCP-1, RAGE and actin are shown. Each lane was loaded with 50 μg protein obtained from the renal cortex. *B*: Intensities of TGF-β protein relative to actin are shown. *E*: Intensities of MCP-1 protein relative to actin are shown. *H*: Intensities of RAGE protein relative to actin are shown. *C and F*: The levels of TGF-β1 mRNA and MCP-1 mRNA detected by real-time PCR. Total RNA was extracted from the renal cortex and subjected to the examination using quantitative real-time PCR. *C*: The amount of TGF-β1 mRNA relative to 18s rRNA is shown. Results are expressed relative to non-diabetic control mice that were arbitrarily assigned a value of 1.0. *F*: The amount of MCP-1 mRNA relative to GAPDH is shown. *B, C, E, F and H:* $^*P < 0.01$ vs. N. $^\dagger P < 0.05$ vs. Ve or LacZ. $n = 5$ for each group.

Fig. 6. *A-E*: Immunoblot analysis (cultured mesangial cells). *A and D*: Immunoblots for MCP-1, TGF-β, RAGE and actin are shown. Each lane was loaded with 20 μg protein obtained from mouse mesangial cells. *B*: Intensities of MCP-1 protein relative to actin are shown. $^*P < 0.05$ vs. NG or NG/Manni. $^\dagger P < 0.05$ vs. HG/V0. $^\ddagger P < 0.05$ vs. HG/V1. *C*: Intensities of TGF-β protein relative to actin are shown. $^*P < 0.05$ vs. NG or NG/Manni. $^\dagger P < 0.05$ vs. HG/V0 or HG/V1. *E*: Intensities of RAGE protein relative to actin are shown. $^*P < 0.05$ vs. NG or NG/Manni. $^\dagger P < 0.05$ vs. HG/V0. $^\ddagger P < 0.05$ vs. HG/V1.

Fig. 7. Double immunofluorescent staining for endogenous mouse VASH-1 (mVASH-1), CD31 and α-SMA. *A:* Double immunofluorescent staining of mVASH-1 (green), CD31 (red) and merged images in the kidney from non-diabetic (upper panels) or diabetic mice (lower panels). Although mVASH-1 was faintly observed in non-diabetic glomeruli, increased immunoreactivity for mVASH-1 was observed, and partially co-localized with the CD31$^+$ endothelial cells (arrowheads), in the control diabetic mice. *B:* Double immunofluorescent staining of mVASH-1 (green), α-SMA (red) and merged images in the kidney from non-diabetic mice (upper panels) or control diabetic animals (lower panels). In the non-diabetic kidney, immunoreactivity for α-SMA was observed in extraglomerular arterioles co-localized with mVASH-1 (arrows). Immunoreactivity of mVASH-1 partially co-localized with the α-SMA$^+$ mesangial cells (arrowheads), in the control diabetic mice. Original magnification x400.

Figure 1

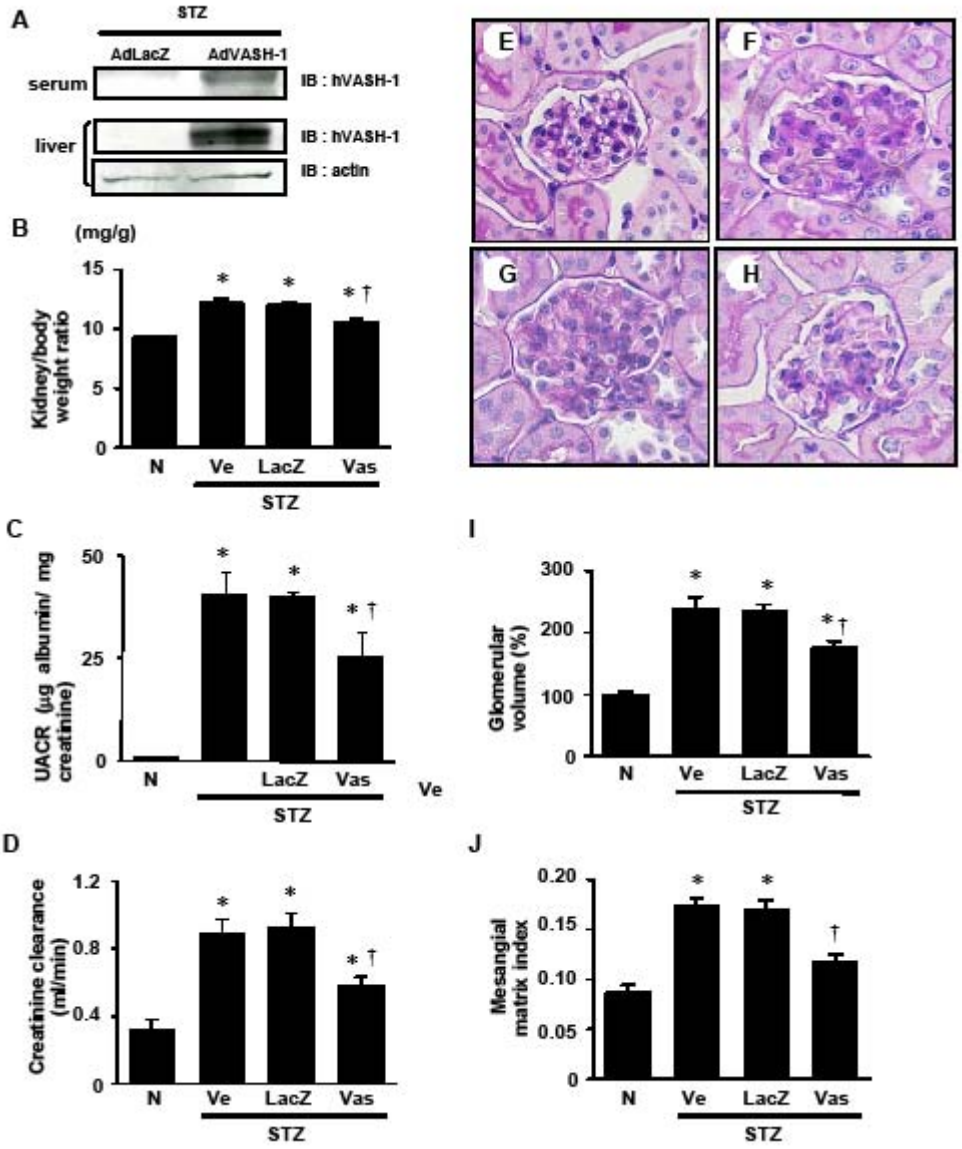
A
STZ
AdLacZ
AdVASH-1
serum
IB : hVASH-1
liver
IB : hVASH-1
IB : actin
B
(mg/g)
Kidney/body weight ratio
15
10
5
0
N
Ve
LacZ
Vas
STZ
E
F
G
H
C
UACR (μg albumin/ mg creatinine)
50
25
0
N
LacZ
Vas
STZ
Ve
I
Glomerular volume (%)
300
200
100
0
N
Ve
LacZ
Vas
STZ
D
Creatinine clearance (ml/min)
1.2
0.8
0.4
0
N
Ve
LacZ
Vas
STZ
J
Mesangial matrix index
0.20
0.15
0.10
0.05
0
N
Ve
LacZ
Vas
STZ

Figure 2

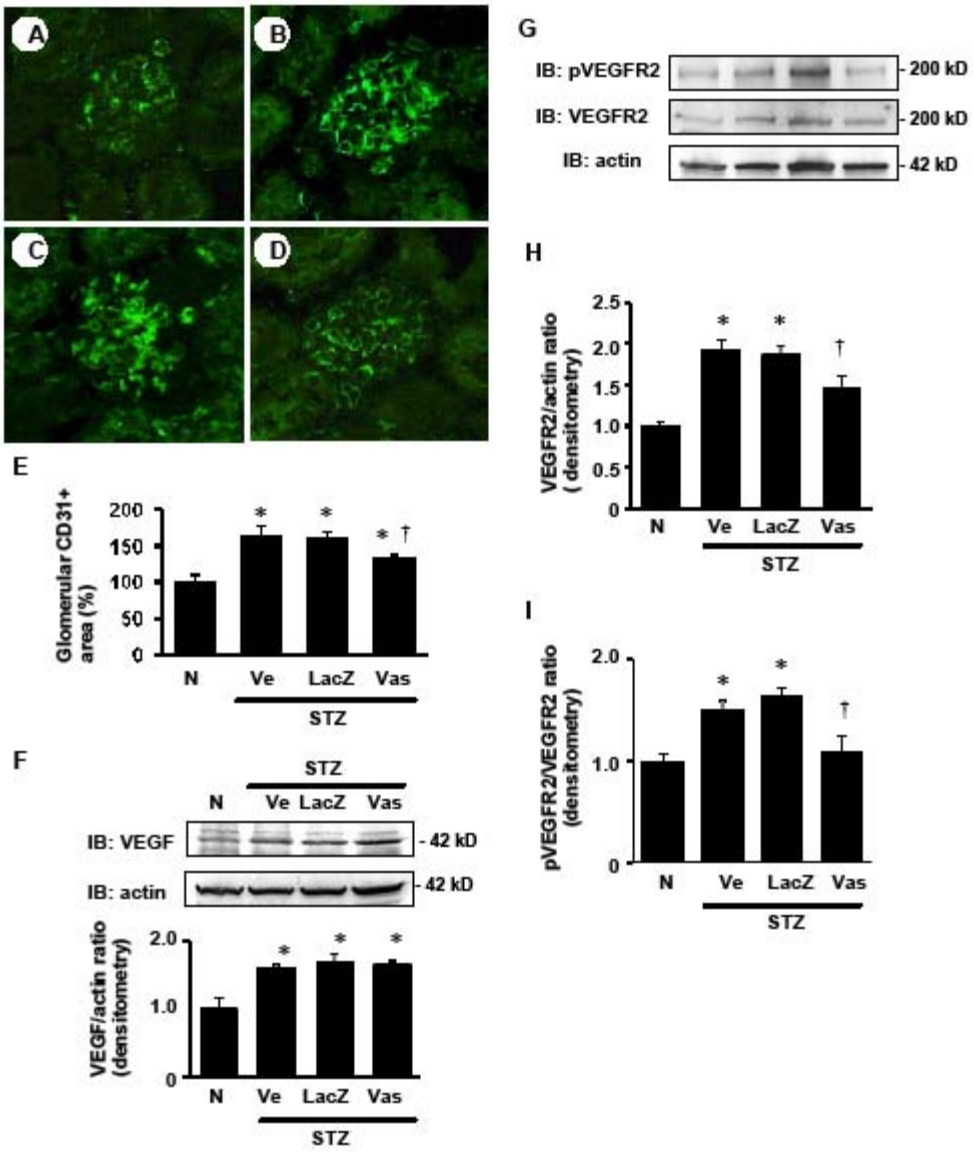
A
B
C
D
E
Glomerular CD31+ area (%)
200
150
100
50
0
N
Ve
LacZ
Vas
STZ
F
STZ
N
Ve
LacZ
Vas
IB: VEGF
42 kD
IB: actin
42 kD
VEGF/actin ratio (densitometry)
2.0
1.0
0
G
IB: pVEGFR2
200 kD
IB: VEGFR2
200 kD
IB: actin
42 kD
H
VEGFR2/actin ratio (densitometry)
2.5
2.0
1.5
1.0
0.5
0
I
pVEGFR2/VEGFR2 ratio (densitometry)

Figure 3

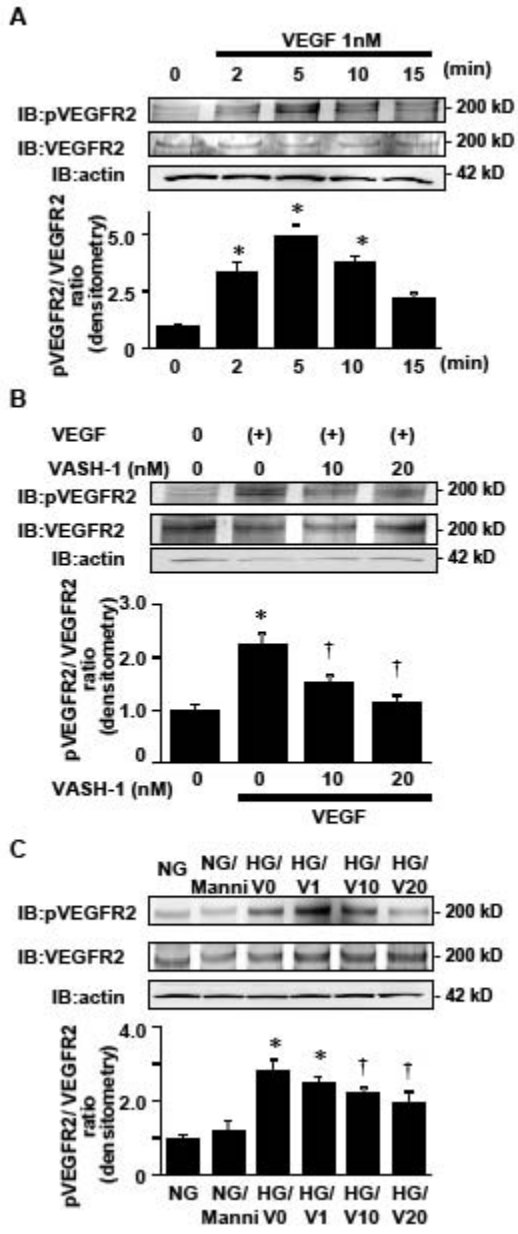
A
VEGF 1nM
0 2 5 10 15 (min)
IB:pVEGFR2
IB:VEGFR2
IB:actin
200 kD
200 kD
42 kD
pVEGFR2/ VEGFR2 ratio (densitometry)
5.0
2.5
0
0 2 5 10 15 (min)
B
VEGF 0 (+) (+) (+)
VASH-1 (nM) 0 0 10 20
IB:pVEGFR2
IB:VEGFR2
IB:actin
200 kD
200 kD
42 kD
pVEGFR2/ VEGFR2 ratio (densitometry)
3.0
2.0
1.0
0
VASH-1 (nM) 0 0 10 20
VEGF
C
NG NG/ Manni HG/ V0 HG/ V1 HG/ V10 HG/ V20
IB:pVEGFR2
IB:VEGFR2
IB:actin
200 kD
200 kD
42 kD
pVEGFR2/ VEGFR2 ratio (densitometry)
4.0
2.0
0
NG NG/ Manni HG/ V0 HG/ V1 HG/ V10 HG/ V20

Figure 4

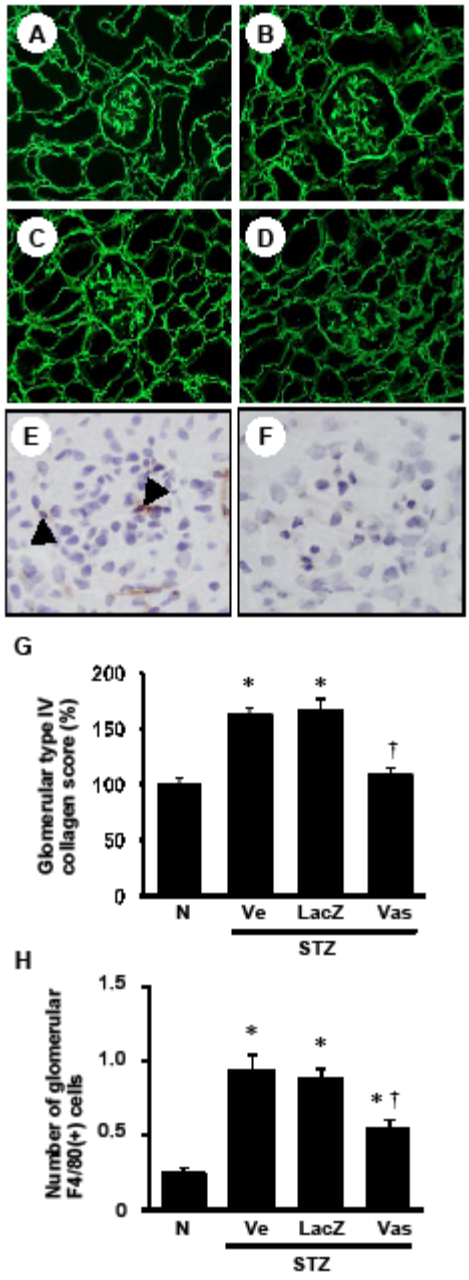
A
B
C
D
E
F
G
Glomerular type IV collagen score (%)
200
150
100
50
0
*
*
†
N
Ve
LacZ
Vas
STZ
H
Number of glomerular F4/80(+) cells
1.5
1.0
0.5
0
*
*
* †
N
Ve
LacZ
Vas
STZ

Figure 5

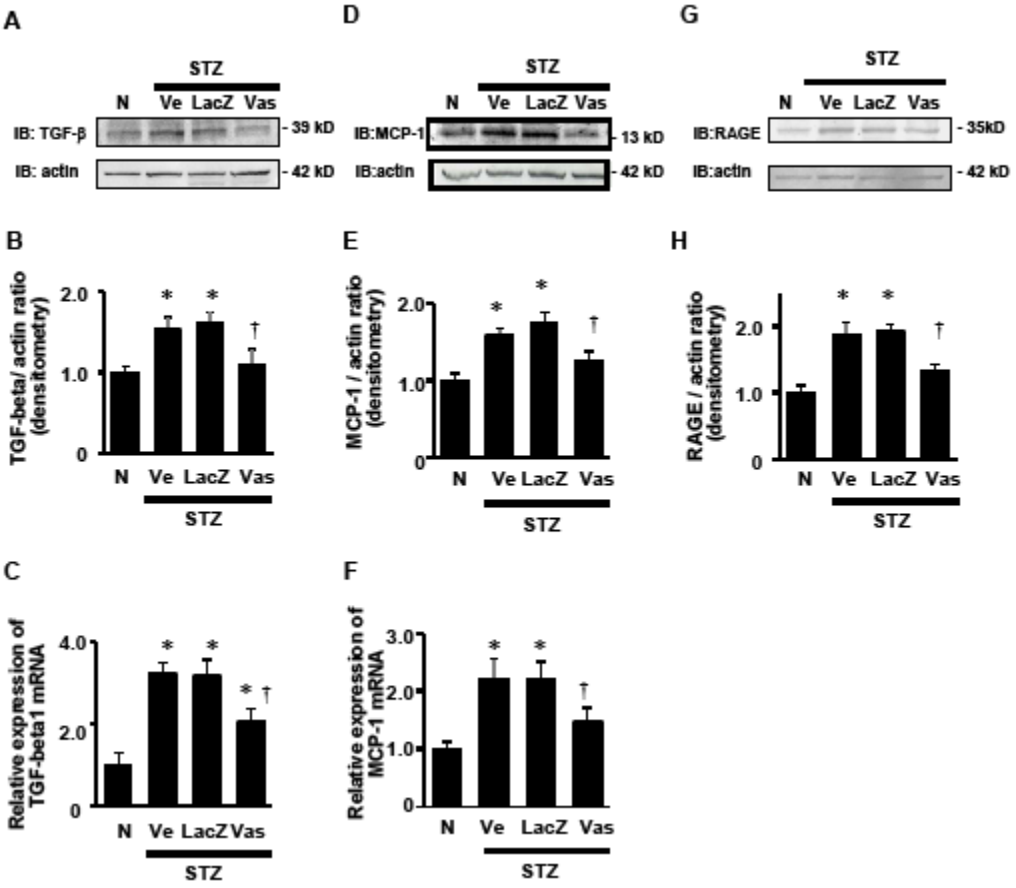
A
STZ
N Ve LacZ Vas
IB: TGF-β
- 39 kD
IB: actin
- 42 kD
D
STZ
N Ve LacZ Vas
IB:MCP-1
- 13 kD
IB:actin
- 42 kD
G
STZ
N Ve LacZ Vas
IB:RAGE
- 35kD
IB:actin
- 42 kD
B
TGF-beta/ actin ratio (densitometry)
2.0
1.0
0
N Ve LacZ Vas
STZ
E
MCP-1 / actin ratio (densitometry)
2.0
1.0
0
N Ve LacZ Vas
STZ
H
RAGE / actin ratio (densitometry)
2.0
1.0
0
N Ve LacZ Vas
STZ
C
Relative expression of TGF-beta1 mRNA
4.0
2.0
0
N Ve LacZ Vas
STZ
F
Relative expression of MCP-1 mRNA
3.0
2.0
1.0
0
N Ve LacZ Vas
STZ

Figure 6

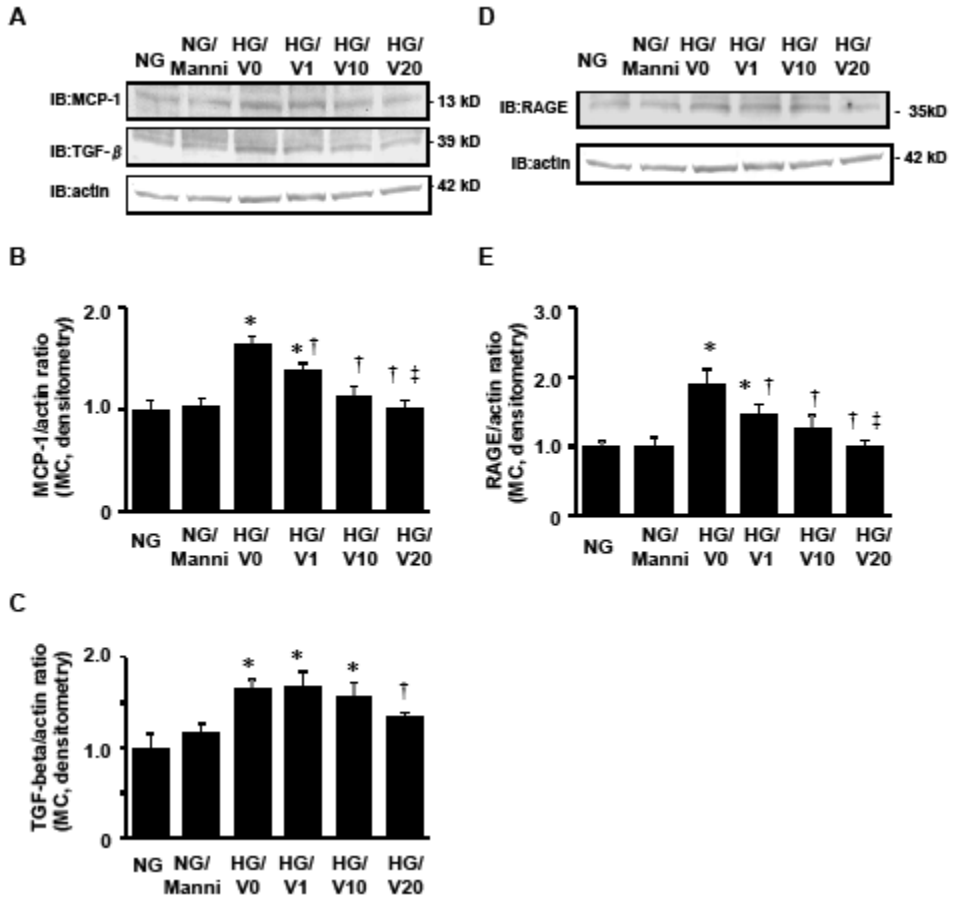
A
NG
NG/ Manni
HG/ V0
HG/ V1
HG/ V10
HG/ V20
IB:MCP-1
13 kD
IB:TGF-β
39 kD
IB:actin
42 kD
D
IB:RAGE
35kD
IB:actin
42 kD
B
MCP-1/actin ratio (MC, densitometry)
2.0
1.0
0
E
RAGE/actin ratio (MC, densitometry)
3.0
2.0
1.0
0
C
TGF-beta/actin ratio (MC, densitometry)
2.0
1.0
0

Figure 7

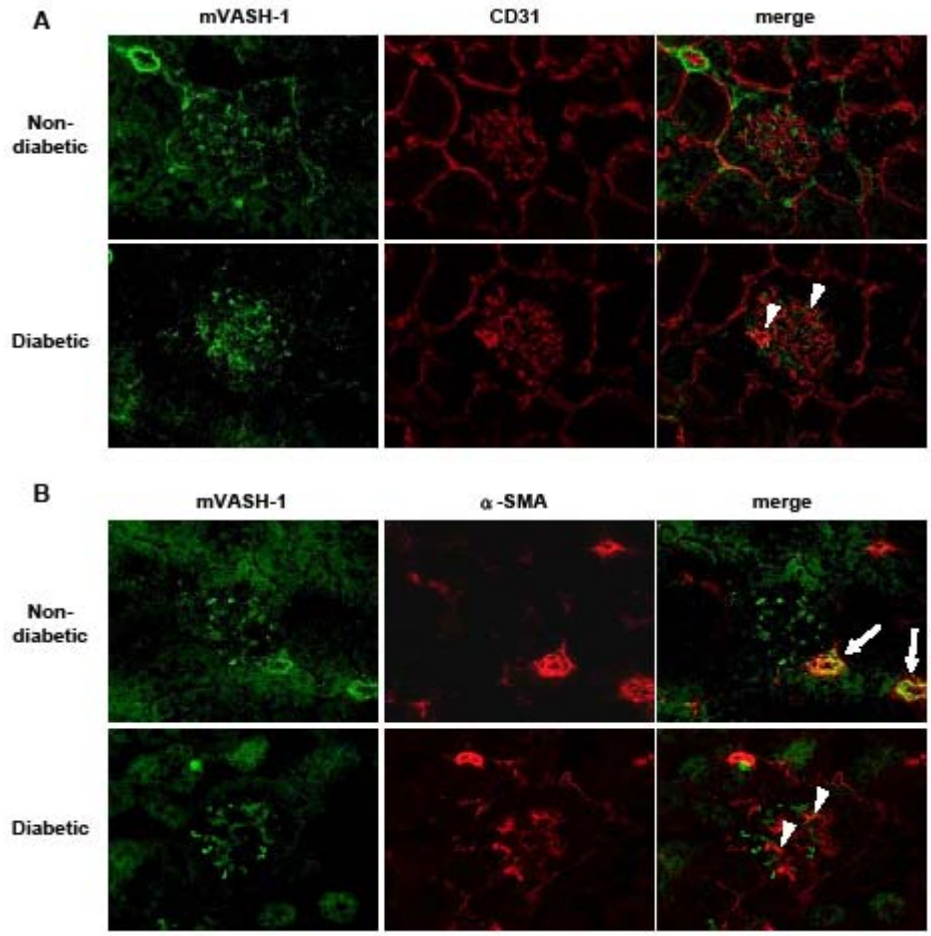
A
mVASH-1
CD31
merge
Non-diabetic
Diabetic
B
mVASH-1
α-SMA
merge
Non-diabetic
Diabetic